

Green Synthesized Iron Nanoparticles from *Tetrapleura tetraptera* for Fluoride Mitigation in Aqueous Media

Abideen Umar Mohammed¹, Ebenezer Annan^{1*}, Grace Karikari Arkorful¹, and Stephen Kofi Armah^{1,2}

¹Department of Materials Science and Engineering, University of Ghana, Legon, Ghana.

²Ashesi University, 1 University Avenue, Berekuso, PMB CT 3, Cantonments Accra, Ghana

*Corresponding author: ebannan@ug.edu.gh

ABSTRACT

The utilization of better remediation methods is required due to the growing concerns of environmental protection and sustainability. In this regard, the use of biosynthesized offers a viable path. This research describes the synthesis of stabilized iron nanoparticles using the fruit of *Tetrapleura tetraptera* as a source of extract. Due to the combination of different phytochemicals confirmed present in the extract through phytochemical screening, reduction and capping of Iron/iron oxide nanoparticles were produced. The change in colour of the extract solution from light brown to dark black verified the presence of iron oxide nanoparticles. X-Ray Diffraction analysis confirmed peaks of Iron/iron oxide nanoparticles and estimated particle size of 30 nm. Fourier Transform Infrared Spectroscopy (FTIR) of both extract and Iron/iron oxide nanomaterial confirmed functional groups associated with the phytochemicals in the extract. The ultra-violet-Visible spectroscopy (UV-Vis) peak of 300 nm was observed which was within the range for iron nanoparticles. Fluoride removal studies show high removal efficiency of 94 % by the iron nanoparticles. kinetic and isotherm modeling undertaken shows that the adsorption occurred by chemisorption on multiple active sites. The results show the successful synthesis of Iron/iron oxide nanoparticles from *Tetrapleura tetraptera* extract and its effect on fluoride removal, therefore providing a sustainable water treatment design system.

Keywords: Fluoride Removal, Green synthesis of magnetite, Water treatment, *Tetrapleura tetraptera*

1.0 INTRODUCTION

Fluoride is naturally embedded in rocks and gets released into water, soil, and air due to volcanic and anthropogenic activities. Major sources of fluoride ingestion by humans are from water, dental products, food, and beverages (Yadav et al. 2007). Fluoride is

non-degradable and its presence in water above accepted limits is detrimental. In drinking water, fluoride levels between 1-1.5 mg/L are favourable to teeth and bones, long exposure to levels above 4 mg/L leads to health risks such as dental and skeletal

fluorosis (Fouladkhah, Thompson, and Camp 2019). As a result, the need for more effective and efficient methods to deal with this problem continues to be a topic of interest for researchers.

The main water treatment methods documented for fluoride reduction include Adsorption (Mondal and George 2015), coagulation, precipitation, ion exchange (Gandhi, Kalaivani, and Meenakshi 2011), electro dialysis (Hichour et al. 1999) and nanofiltration (Simons 1993). However, adsorption has been documented as the most favorable because of its cost effectiveness, simple and an environmentally friendly approach (Onyango and Matsuda 2006). It is important to note that most of these adsorption processes are being engineered for real-life application. Among the different materials (activated and impregnated alumina, hydroxyapatite, quick lime, hydrated cement activated carbon, waste residue, ion-exchanger, various types of activated clay, impregnated silica, and plaster of Paris) reported to have been used for fluoride removal, metal nanoparticles have shown far greater performance. The comparative high removal efficiency by metal nanoparticles is due to their excellent magnetic, physical, optical, electrical, and chemical properties which differ marginally from most materials including their bulk counterparts (Liang et al. 2021).

In recent years, nanotechnology has become a cutting-edge technology in microbiology, optics,

environmental remediation, and various engineering applications. It involves nanoparticles which are materials with reduced size and high surface area to volume ratio, higher stability, biological compatibility, high reactivity, and photocatalytic activity making them the perfect photocatalyst for fluoride removal and other environmental remedies (Bishnoi, Kumar, and Selvaraj 2018). For specific defluorination purposes, various metal and metal oxide-based nanoparticles have been utilized to study their removal efficiencies but unfortunately, they require expensive centrifuging for separation. Iron and iron oxide nanoparticles (FeNPs/FeONPs) on the other hand are easy to separate with excellent recoverability, reactivity, and photocatalytic properties (Annan et al. 2021). Additionally, iron is abundant and therefore the most suitable nanoparticles for environmental remediation (O'Carroll et al. 2013). Bulk iron oxide and iron oxide nanoparticle has been reported to give moderate adsorption of fluoride in water and its nanoparticle reportedly removed fluoride completely (Deliyanni et al. 2004) (Zhao et al. 2016). The removal efficiency or performance of iron nanoparticles depends on the size and morphology. Chemical synthesis techniques such as chemical reduction, sol gel process, co-precipitation, hydrothermal synthesis (McNeil 2005) involve the use of toxic reagents such as hydrazine hydrate (Adhikari et al. 2020),

N N-dimethylformamide (Aryal et al. 2019), and the borohydride and/or hydroxide of sodium as reducing agents (Adhikari et al. 2020), N N-dimethylformamide (Aryal et al. 2019), and the borohydride and/or hydroxide of sodium as reducing agents for the synthesis of nanoparticles and, form hazardous by-products (Jing et al. 2020). This has led to research into sustainable or green, less expensive, and less sophisticated approaches over the past decade (Jadoun et al. 2021; Ying et al. 2022). Synthesis of FeNPs via plant sources offers significant benefits over other biological techniques in terms of simplicity and cost, with the reduction of precursors occurring at a faster rate. The presence of a plethora of poly-phenolic compounds in the plant extracts affords them the ability to cap the individual nanoparticles, simultaneous reduction and stabilization during the synthesis of nanoparticles (Izadiyan et al. 2020).

In the last decade, green synthesis has been the sustainable approach adopted by many researchers. Published research works have proven the successful synthesis of Iron nanoparticles (FeNps) and Iron Oxide nanoparticles (FeONPs) using leaves and fruits of plants such as *Carica papaya*, *Persea americana*, *Punic granatum*, and leaves of *Tetrapleura tetraptera*, etc (Ogunsile, Seyinde, and Salako 2020; Castillo-Henríquez et al. 2020; Bouafia and Laouini 2021). Silver nanoparticles has been green synthesized from *Tetrapleura tetraptera* (Ogunsile, Seyinde, and Salako 2020).

Tetrapleura tetraptera is a flowering plant which belonging to the family *Fabaceae* and mostly found in West African countries. It has been reported to contain several phytochemicals which include, tannins, flavonoids, and starch which enables them to reduce iron salts and are able to adequately cap metal nanoparticles because of their numerous hydroxyl groups which confer on them higher reduction potential and chelating powers. This research adopts green approach in the synthesis of iron nanoparticles (FeNPs) from *Tetrapleura tetraptera* extract and examine its efficacy in the removal of fluoride from aqueous media.

2.0 MATERIALS AND METHODS

The reagents used in this research were all analytical grade and were supplied by Sigma-Aldrich. The reagents used include: 0.1 M hydrochloric acid (HCl), sodium hydroxide (NaOH), ferric chloride (FeCl₃), ethanol (C₂H₆O), chloroform (CHCl₃), sodium ferrocyanide [Fe(CN)₆]⁴⁻ and sulfuric acid (H₂SO₄). Fluoride solution was prepared from 22.2 mg of sodium fluoride. TISAB 1 solution was used to dissolve any complexes of the fluoride prior reading of UV-Vis. Fluoride concentrations were measured using Iron Selective Electrode HI4110 (HANNA Instruments, Inc., Woonsocket, USA)

2.1. Extract Preparation and Screening

The fruits of *Tetrapleura tetraptera* were purchased from a local market in Accra, Ghana. *Tetrapleura tetraptera* fruit sample was washed with water, dried under the sun for a week and further dried in an oven at 60 °C for the removal of any excess moisture. The dried fruits were pulverized and sieved into particle size of 150 microns. A solution of Ethanol and water was made in a ratio of 2:1 to obtain a total volume of 750 mL. A mass of 166.9 g of the powdered *Tetrapleura tetraptera* sample was added to the ethanol-water mixture in a beaker. The mixture in the beaker was heated at 60° C for an hour at constant stirring speed of 700 rpm. Following the settlement of mixture, the mixture was filtered using a filter paper (150 microns) to obtain liquid portions and stored in a refrigerator. The flow diagram for the process is provided in supplementary information 1(SI 1).

Phytochemical screening was undertaken to ascertain their availability in the *Tetrapleura tetraptera* extract. Chemical structures for some of the phytochemicals are in supplementary information 2 (SI 2). Braymer's test for tannin was conducted where 20 mL the plant extract was diluted with 5 mL of distilled water. The diluted extract solution was heated, filtered, and 2 mL ferric chloride solution was added dropwise. A change of colour from light brown to blue-black confirms the availability of tannin. In a ferric chloride test for

polyphenols, few drops of 0.1M ferric chloride solution was added to 5 mL of the extract. Positive result is confirmed by the appearance of a blue colouration for the ferric chloride test. Salkowki's test for terpenoid was also conducted. For this, 5 mL of the extract, 5 mL of H₂SO₄ solution and 2.5 mL of chloroform were mixed, where the appearance of a reddish-brown layer signifies a result for terpenoid. The flavonoid test was undertaken by adding 5ml of dilute NaOH and by 5mL of HCl to a tube containing 2.5 mL of the extract in an alkaline reagent. Colour change from yellow to colourless shows presence of flavonoids. The experimental process for nanoparticles synthesis and the colour changes of the solutions are provided in supplementary information 3(SI 3) and supplementary information 4(SI 4) respectively.

2.3. Characterization

FTIR analysis was undertaken on powdered dried fruit samples and iron nanoparticle solution to study the chemical bonds present in the phytochemicals which are responsible for the reduction of iron. X-ray diffraction (XRD) analysis was run on the powdered iron oxide nanoparticles to study the crystallographic nature of the iron oxide nanoparticles. Ultraviolet-visible spectroscopy (UV-Vis) of the synthesized iron nanoparticle solution was obtained.

2.4 Batch adsorption Experiment

The batch adsorption experiment as carried out using 5 mg, 10 mg and 14 mg of the adsorbent and 15 mg of the adsorbent and added to 250 ml of the adsorbate. To ensure uniform mixing, orbital shaker was used at constant speed of 250 rpm. The concentrations of fluoride were determined for each contact time and for each adsorbent dosage. The removal efficiency values, kinetic and isotherm modelling plots were analysed to fully describe the adsorption mechanism. Adsorption capacity and removal efficiency equations are represented in equations (1) and (2) respectively.

$$q=(C_o-C_t)\frac{V}{m}, \quad (1)$$

$$A\%=\left(\frac{C_o-C_t}{C_o}\right)\times 100 \quad (2)$$

where 'v' represents the volume of the solution, m represents adsorbent dosage, C_o represents initial concentration of fluoride ions and C_t represents the fluoride concentration at any given time(t)

3.0 RESULTS AND DISCUSSIONS

3.1. Phytochemical screening

Polyphenols, flavonoids, saponins and tannins were all present in the extract of the *Tetrapleura tetraptera*. A negative test result was obtained for terpenoids as presented as indicated in Table1. However, this has no significant effect on the reduction process because polyphenols confirmed to be available in the extract are the most prominent phytochemicals for capping and stabilization of iron nanoparticles (Bouafia and Laouini 2021).

Flavonoids also have good reduction and complexing properties aided by hydroxyl groups present in their structure (Bouafia and Laouini 2021). The proof of these phytochemicals' presence in the extract indicates the collective reducing properties which aided in the capping of Fe^{3+} ions and stabilization of iron nanoparticles.

Table 1: Phytochemical screening of *Tetrapleura tetraptera* extracts

Phytochemical	TEST Results
Polyphenols	Positive
Saponin	Positive
Flavonoid	Positive
Tannin	Positive
Terpenoids	Negative

3.2. Synthesis of Iron Nanoparticles (FeNps)

The extract solution upon addition of FeCl_3 solution changed color to deep black implying the capping of the precursor iron solution and formation of nanomaterials. This confirms collective reduction by the different phytochemicals present in the extract. Additionally, the development of a stable, dark colored colloidal solution that did not alter over time showed that there were enough nucleation agents present to control the production of nanoparticles (SI 3 and SI 4).

3.3. Characterization of extract and FeNps

The most popular and accepted method being utilized to describe the optical characteristic of nanomaterials is UV-Vis absorption spectroscopy. The surface plasmon resonance band of nanomaterials gives an idea about their morphology (Guo et al. 2020). The green synthesized nanoparticles showed a maximum peak at 300 nm which indicate that, the green synthesized nanoparticles absorbs the UV light and it's a characteristic surface plasmon resonance band for metallic iron nanoparticles (Shafey 2020; Kiwumulo et al. 2022). Figure 1(a) and Figure 1(b) shows the UV-Vis

spectroscopy and X-ray diffraction studies spectra of the synthesized iron nanoparticles respectively.

The crystallography of the powdered nanomaterial was studied via XRD studies. The peaks from figure 1(b) were observed at $2\theta = 22.1^\circ, 29.4^\circ, 36.2^\circ, 39.4^\circ$ and 47.3° corresponded to cubic (220), (311), (400), (422) and (511) crystal planes of Fe_3O_4 nanoparticles (Shafey 2020). Machado et al have reduced Fe^{3+} to zero-valent FeNPs and observed predominant peak at $2\theta = 46^\circ$ (Machado et al. 2015). The peak at $2\theta = 46^\circ$ which signifies capping of iron nanoparticles to the zero-valent iron was absent and proposed that the absence was due to coating of the iron core by compounds from the extract rendering it undetectable. Average particle size was of 30 nm as estimated from the Scherrer's equation (Chaki et al. 2015):

$$D = \frac{K\lambda}{\beta \cos\theta}, \quad (3)$$

where D = crystalline size, $K = 0.9$ (Scherrer constant), $\lambda = 0.15673$ nm, β = Full Width at Half Minimum (radians) and θ represents Peak Position (radians).

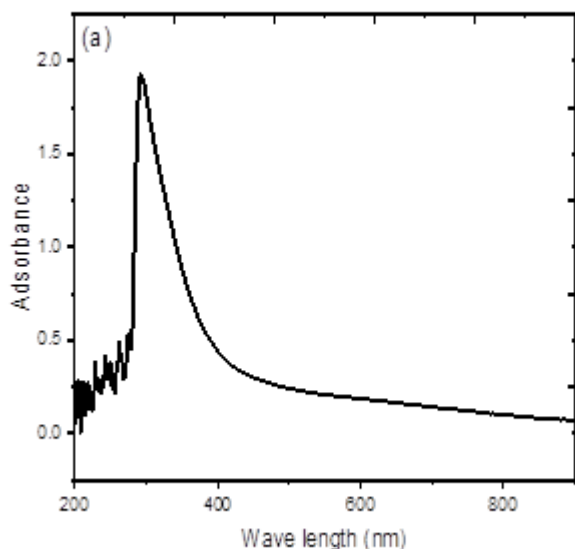


Figure 1(a): UV-Vis Spectrum for FeNps,

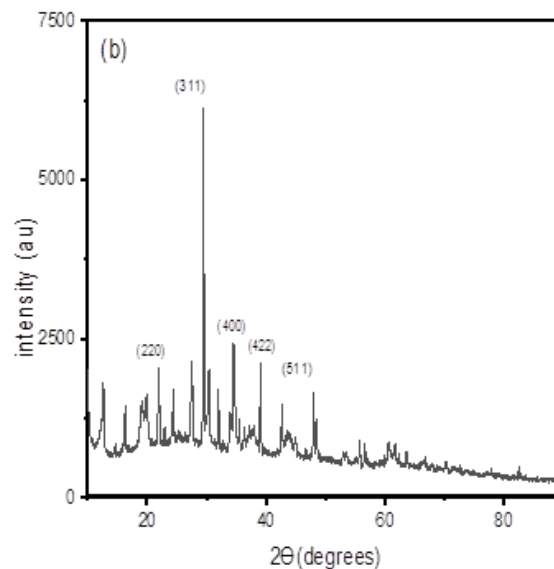


Figure 1(b): XRD spectrum for FeNps.

Table 2 (a) Absorption bands from FTIR spectrum of *Tetrapleura tetraptera* extract and their functional groups.

Wavelength (cm ⁻¹)	Functional Groups
3302	O-H (hydroxyl group)
2921	C-H and CH ₂ (aliphatic Hydrocarbon)
1602	C=C (ketone)
1047	C-O (alcohol stretch)

Table 2 (b) Absorption bands for FeNp spectrum and their functional groups

Wavelength (cm ⁻¹)	Functional Group
3394	O-H
2921	C-H & CH ₂
1602	C=C
1098	C-O

FTIR spectra for both the extract and FeNPs possessed similar functional groups with slight differences in absorption peaks and intensities as shown in Tables 2(a) and 2(b) respectively (complemented by Figure 2). The extract and nanoparticles displayed comparable adsorption bands which might be explained by the fact that the main phytochemicals in the extract have identical functional groups. These represent the predominant functional groups associated with the dominant phytochemicals available in the extract for the capping and stabilization of iron nanoparticles.

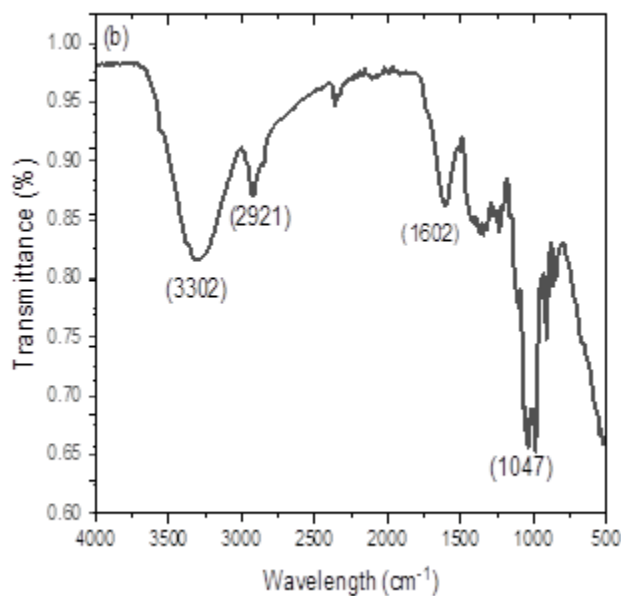
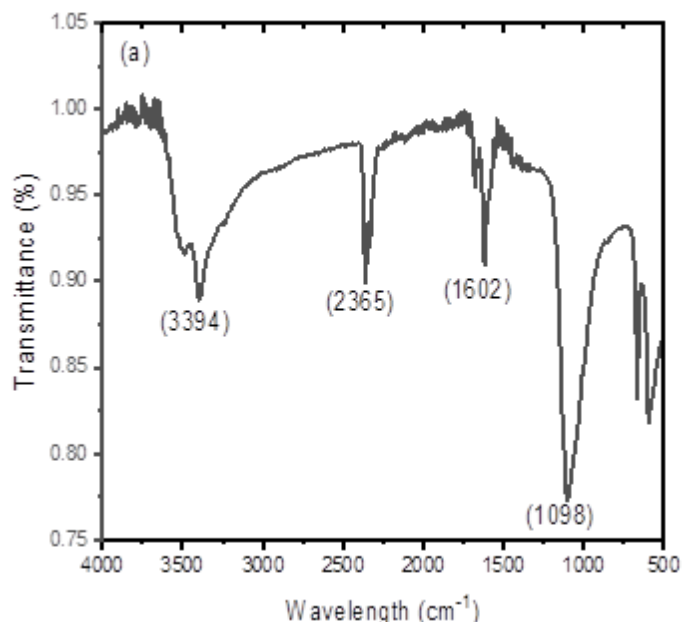


Figure 2: FTIR plot for (a) *Tetrapleura tetraptera* Extract, (b) FeNp

3.4. Effect of Dosage and Time

Fluoride removal efficiency as time varies for the three doses of the synthesized nanoparticles were plotted (Figure 3). The average removal percentages for 5 mg, 10 mg and 15 mg adsorbent were 42%, 64%, and 81% respectively. For the three different doses, as contact time was increased, defluorination also increased until maximum removal percentages for the 5 mg, 10 mg, and 15 mg which were 62%, 83% and 94% respectively were reached at 180 minutes. This has been explained to be due to numerous vacant sites initially available when the adsorbate concentrations are high (Annan et al. 2021; Appiah et al. 2022). The removal efficiency values are observed to hardly vary from a fixed value, indicating that the adsorption process has reached equilibrium. This may be due to lack of any more active sites for either recombination or adherence.

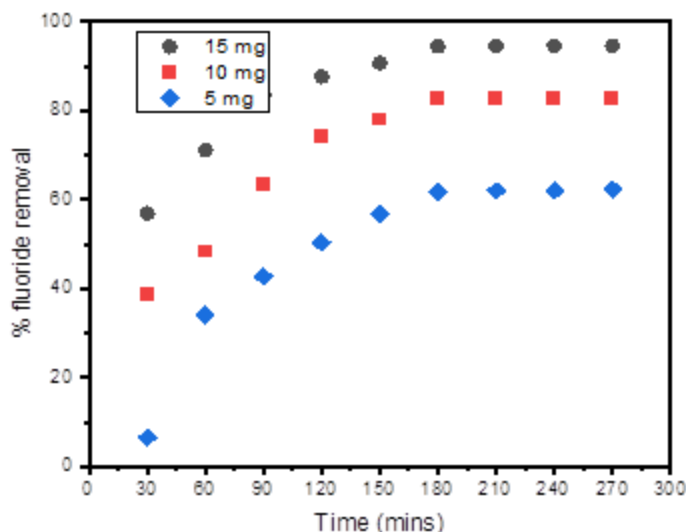


Figure 3: Effect of contact time on removal efficiency

There could also be reduced adsorbate for remaining available site. In the latter case, further agitation, depending on the type and strength of the binding/adherence to the active site, may detach and recombination may occur later. In this research, higher dose was found to show more adsorption capability than lower doses at all the contact times investigated. For each dose, gradual increase is observed as time in contact prolongs.

3.5 Kinetic and Isotherm Model

The adsorption data for the adsorbent doses were fit to the pseudo- first order (equation 4) and pseudo-second order (equation 5) kinetic models as shown in figure 8. The rate of solute uptake is described by the process of kinetics, which in turn enables the specific level of defluorination to be determined.

$$\log(q_e - q_t) = \log q_e - \frac{K_1}{2.303} t, \quad (4)$$

$$\frac{t}{q_t} = \frac{1}{(k_2 q_e^2)} + \frac{t}{q_e}, \quad (5)$$

Table 3.0 shows the values for estimated parameters for kinetic modeling analysis. The plots fitted to the models are provided in supplementary information, SI 5. The use of R-square (R²) is the popular and accepted approach in determining better fit. The Pseudo- second order had higher R² value than the pseudo-first order. This implies that removal of fluoride ions by the synthesized nanomaterial is characterized by chemical adsorption which involves ion exchanges (Appiah et al. 2022; Annan et al. 2021). The fundamental principles describing the mechanism for the adsorption process was explained in the current work using the Langmuir (equation 6) and Freundlich (equation 7) models. Langmuir model assumes that the adsorption occurs on a monolayer. This is due to the assumption that the adsorption sites on the surface of the adsorbent have comparable affinities for only one molecule of the adsorbate. Also, concentration difference between sites of proximity does not affect rate of adsorption (Habuda-Stanić, Ergović Ravančić, and Flanagan 2014). The Freundlich model is empirical, and it assumes that adsorption occurs on a multilayer. This imposes availability of numerous dissimilar active sites for adsorption.

Original form: $q_e = \frac{q_m K_L C_e}{1 + K_L C_e}$, (6) Adsorption mechanism is influenced by the Langmuir model when separation factor (K_L) is within the range of $0 < K_L < 1$. However, when and the heterogeneity factor (n) is greater than 1, the Freundlich isotherm model is favoured. From the experimental results in Table 4, it was found that the heterogeneity factor (n) for the three adsorbent masses was greater than 1.

Linearized form: $\frac{C_e}{q_e} = \frac{1}{K_L q_m} + \frac{1}{q_m} \times C_e$

Original form: $q_e = K_F \times C_e^{1/n}$ (7)

Linearized form: $\log q_e = \log K_F + \frac{1}{n} \log C_e$

Table 3: Kinetic models’ parameters for adsorption of fluoride.

Adsorbent Mass(mg)	Pseudo First Order (PFO)			Pseudo Second Order (PSO)		
	K_1 (min^{-1})	q_e (mg/g)	R^2	K_2 (g/mg/min)	q_e (mg/g)	R^2
5.0	0.087	0.37	0.94	15.68	0.40	0.97
10.0	0.091	0.25	0.96	13.77	0.27	0.98
15.0	0.116	0.19	0.95	11.36	0.20	0.99

Table 4: Adsorption isotherm model parameters for adsorption of fluoride

Adsorbent Mass (mg)	Langmuir Model			Freundlich Model		
	K_L (L/mg)	q_{max} (mg/L)	R^2	K_F (mg/g)	n	R^2
5.0	11.66	0.44	0.90	0.042	5.47	0.99
10.0	21.81	0.25	0.82	0.082	6.13	0.98
15.0	29.55	0.18	0.98	0.015	6.86	0.995

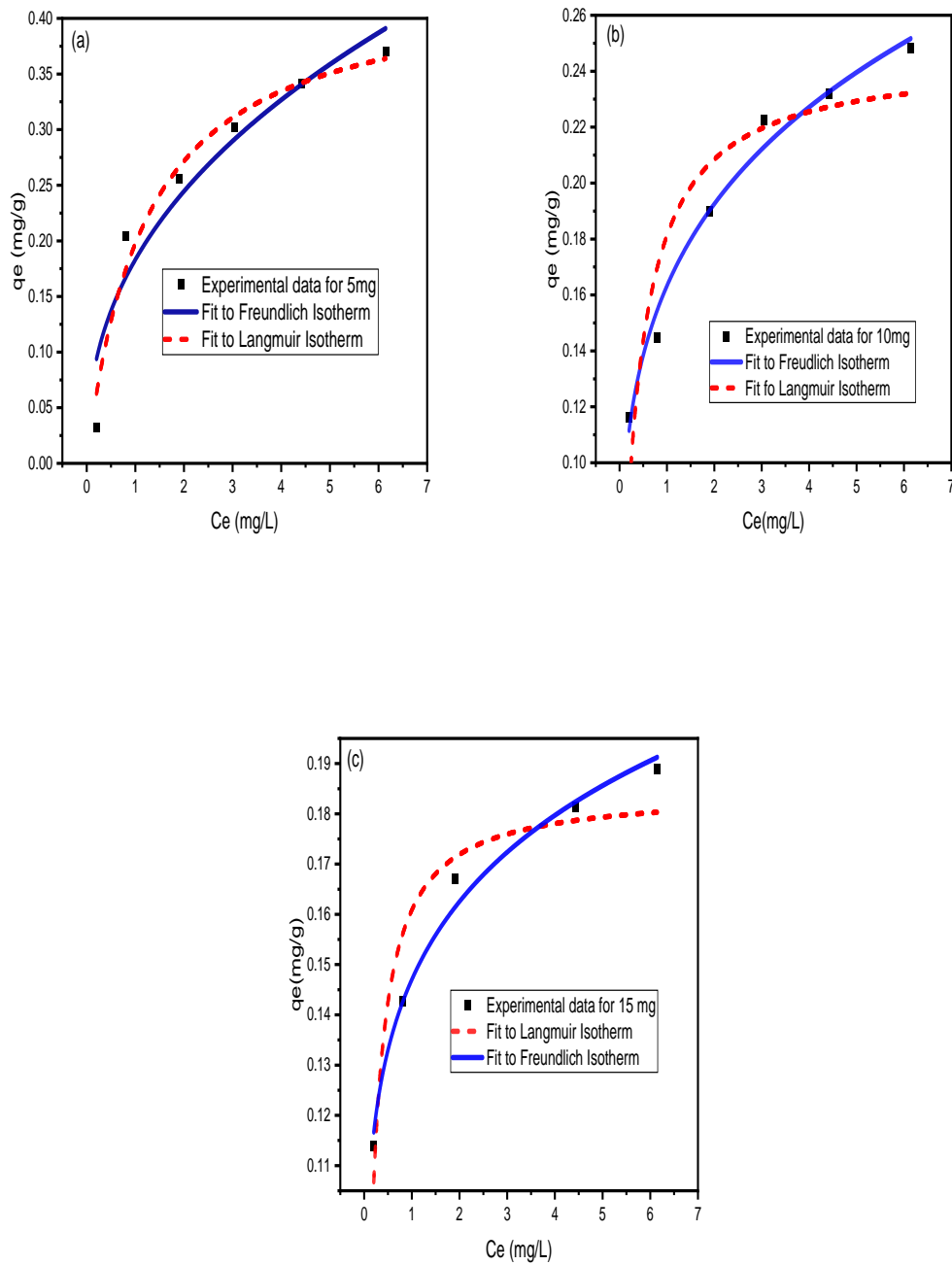


Figure 4: Isotherm modelling for (a) 5mg, (b) 10 mg and (c) 15 mg adsorbent.

4.0 CONCLUSION

Iron nanoparticles were successfully synthesized using the fruits of *Tetrapleura tetraptera*. Plant Phytochemicals acted as aided reducing agent of Fe^{3+} ions from the precursor solution to metallic FeNps. The most essential phytochemicals for capping and stabilizing the iron nanoparticles, polyphenols (with hydroxyl groups) were confirmed present from the FTIR analysis. Other predominant functional groups were also confirmed and aided in the collective reduction process. The FeNps showed a significant removal efficiency of 94 % towards the fluoride ions in the aqueous media. The kinetic process for fluoride adsorption by FeNps suits the pseudo-second order which implies chemisorption of fluoride ions. The experimental results suggest that the adsorption process fits Freundlich adsorption model implying that adsorption occurred on a multilayer. Therefore, the synthesized FeNps have proven to be very good candidate for the treatment of fluoride contaminated water. Further work should be undertaken on the further characterization of FeNps using Transmission Electron microscopy, regeneration undertaken, and reuse of the FeNps. Also, functionalization of the nanoparticles to investigate it efficacy towards other contaminants are equally paramount.

REFERENCES

- Adhikari, Menuka, Elena Echeverria, Gabrielle Risica, David N McIlroy, Michael Nippe, and Yolanda Vasquez. 2020. 'Synthesis of Magnetite Nanorods from the Reduction of Iron Oxy-Hydroxide with Hydrazine', *ACS omega*, 5: 22440-48.
- Annan, Ebenezer, Emmanuel Nyankson, Benjamin Agyei-Tuffour, Stephen Kofi Armah, George Nkrumah-Buandoh, Joanna Aba Modupeh Hodasi, and Michael Oteng-Peprah. 2021. 'Synthesis and characterization of modified kaolin-bentonite composites for enhanced fluoride removal from drinking water', *Advances in Materials Science and Engineering*, 2021: 1-12.
- Appiah, Augustine Nana Sekyi, Lucas Nana Wiredu Damoah, Yaw Delali Bensah, Peace Korshiwor Amoatey, Daniel Nukpezah, Aubin Aholouvi, and Ebenezer Annan. 2022. 'Evaluation of adsorption properties of organic wastes in aqueous media for arsenic removal', *International Journal of Energy and Environmental Engineering*: 1-11.
- Aryal, Susmita, Hyungkyu Park, James F Leary, and Jaehong Key. 2019. 'Top-down fabrication-based nano/microparticles for molecular imaging and drug delivery', *International journal of nanomedicine*: 6631-44.

- Bishnoi, Shahana, Aarti Kumar, and Raja Selvaraj. 2018. 'Facile synthesis of magnetic iron oxide nanoparticles using inedible *Cynometra ramiflora* fruit extract waste and their photocatalytic degradation of methylene blue dye', *Materials Research Bulletin*, 97: 121-27.
- Bouafia, Abderrhmane, and Salah E Laouini. 2021. 'Plant-mediated synthesis of iron oxide nanoparticles and evaluation of the antimicrobial activity: A review', *Mini-Reviews in Organic Chemistry*, 18: 725-34.
- Castillo-Henríquez, Luis, Karla Alfaro-Aguilar, Jeisson Ugalde-Álvarez, Laura Vega-Fernández, Gabriela Montes de Oca-Vásquez, and José Roberto Vega-Baudrit. 2020. 'Green synthesis of gold and silver nanoparticles from plant extracts and their possible applications as antimicrobial agents in the agricultural area', *Nanomaterials*, 10: 1763.
- Chaki, SH, Tasmira J Malek, MD Chaudhary, JP Tailor, and MP Deshpande. 2015. 'Magnetite Fe₃O₄ nanoparticles synthesis by wet chemical reduction and their characterization', *Advances in Natural Sciences: Nanoscience and Nanotechnology*, 6: 035009.
- Deliyanni, E, D Bakoyannakis, A Zouboulis, and K Matis. 2004. 'Development and study of iron-based nanoadsorbents', *Journal of Mining and Metallurgy B: Metallurgy*, 40: 1-9.
- Fouladkhah, Aliyar Cyrus, Brian Thompson, and Janey Smith Camp. 2019. 'Safety of food and water supplies in the landscape of changing climate.' In, 469. MDPI.
- Gandhi, M Rajiv, Govindasamy Kalaivani, and S Meenakshi. 2011. 'Sorption of chromate and fluoride onto duolite a 171 anion exchange resin—a comparative study', *Elixir Pollution*, 32: 2034-40.
- Guo, Yuchen, Chunhong Liu, Rongke Ye, and Qingling Duan. 2020. 'Advances on water quality detection by uv-vis spectroscopy', *Applied Sciences*, 10: 6874.
- Izadiyan, Zahra, Kamyar Shamel, Mikio Miyake, Hirofumi Hara, Shaza Eva Binti Mohamad, Katayoon Kalantari, Siti Husnaa Mohd Taib, and Elisa Rasouli. 2020. 'Cytotoxicity assay of plant-mediated synthesized iron oxide nanoparticles using *Juglans regia* green husk extract', *Arabian Journal of Chemistry*, 13: 2011-23.
- Jadoun, Sapana, Rizwan Arif, Nirmala Kumari Jangid, and Rajesh Kumar Meena. 2021. 'Green synthesis of nanoparticles using plant extracts: A review', *Environmental Chemistry Letters*, 19: 355-74.

- Jing, Feng, Bai Hui, Xue Yudan, Zhang Rui, Zhu Puli, Bu Duo, Dan Zeng, Li Wei, and Lu Xuebin. 2020. 'Recycling of iron and aluminum from drinking water treatment sludge for synthesis of a magnetic composite material (ALCS-Fe-Al) to remove fluoride from drinking water', *Groundwater for Sustainable Development*, 11: 100456.
- Kiwumulo, Henry Fenekansi, Haruna Muwonge, Charles Ibingira, Michael Lubwama, John Baptist Kirabira, and Robert Tamale Ssekitoleko. 2022. 'Green synthesis and characterization of iron-oxide nanoparticles using *Moringa oleifera*: a potential protocol for use in low and middle income countries', *BMC Research Notes*, 15: 1-8.
- Liang, Li, Weiyang Li, Yue Li, Wei Zhou, and Jiping Chen. 2021. 'Removal of EDTA-chelated CdII by sulfidated nanoscale zero-valent iron: Removal mechanisms and influencing factors', *Separation and Purification Technology*, 276: 119332.
- Machado, S, JG Pacheco, HPA Nouws, José Tomás Albergaria, and Cristina Delerue-Matos. 2015. 'Characterization of green zero-valent iron nanoparticles produced with tree leaf extracts', *Science of the total environment*, 533: 76-81.